PHYSICAL REVIEW C **87**, 014302 (2013)

Investigation of the ^{243}Am + ^{48}Ca reaction products previously observed in the experiments on elements 113, 115, and 117

Yu. Ts. Oganessian,[1,*] F. Sh. Abdullin,[1] S. N. Dmitriev,[1] J. M. Gostic,[2] J. H. Hamilton,[3] R. A. Henderson,[2] M. G. Itkis,[1] K. J. Moody,[2] A. N. Polyakov,[1] A. V. Ramayya,[3] J. B. Roberto,[4] K. P. Rykaczewski,[4] R. N. Sagaidak,[1] D. A. Shaughnessy,[2] I. V. Shirokovsky,[1] M. A. Stoyer,[2] N. J. Stoyer,[2] V. G. Subbotin,[1] A. M. Sukhov,[1] Yu. S. Tsyganov,[1] V. K. Utyonkov,[1] A. A. Voinov,[1] and G. K. Vostokin[1]

[1]*Joint Institute for Nuclear Research, RU-141980 Dubna, Russian Federation*

[2]*Lawrence Livermore National Laboratory, Livermore, California 94551, USA*

[3]*Department of Physics and Astronomy, Vanderbilt University, Nashville, Tennessee 37235, USA*

[4]*Oak Ridge National Laboratory, Oak Ridge, Tennessee 37831, USA*

(Received 9 September 2012; revised manuscript received 16 October 2012; published 3 January 2013)

Results from the production and decay properties of element 115 nuclei observed using the reaction ^{243}Am + ^{48}Ca at various beam energies between November 1, 2010, and February 26, 2012, at the Dubna Gas Filled Recoil Separator are presented. This long-running experiment with a total beam dose of 3.3×10^{19} and carried out in the excitation energy range $E^* = 31$–47 MeV of the ^{291}115 compound nucleus resulted in observation of three isotopes of element 115 with masses 287, 288, and 289. The 28 detected decay chains of ^{288}115 show that this isotope is produced with the maximum probability at $E^* = 34.0$–38.3 MeV with a corresponding cross section of $\sigma_{3n} = 8.5^{+6.4}_{-3.7}$ pb. The four events attributed to the isotope ^{289}115 that decays via a short $\alpha \rightarrow \alpha \rightarrow$ SF chain could be detected only at the lowest excitation energy $E^* = 31$–36 MeV, in accordance with what could be expected for the 2n-evaporation channel of the reaction. The decay characteristics of this nuclide were established earlier (2010) and more recently (2012) in the reaction ^{249}Bk(^{48}Ca,4n)^{293}117 and following α decay to ^{289}115. At the energy $E^* = 44.8 \pm 2.3$ MeV we observed only a single long chain of the isotope ^{287}115. The decay properties of nuclei starting at ^{288}115 and ^{287}115 isotopes obtained in the present work reproduce in full the results of the first experiment of 2003 that reported the discovery of elements 115 and 113. The excitation functions of the production of the isotopes of element 115 and observation of the isotope ^{289}115 in cross-bombardment reactions with the targets of ^{243}Am and ^{249}Bk provide additional evidence of the identification of the nuclei of elements 115 and 113. The experiments were carried out using the ^{48}Ca beam of the U400 cyclotron of the Flerov Laboratory of Nuclear Reactions, JINR.

DOI: 10.1103/PhysRevC.87.014302 PACS number(s): 27.90.+b, 23.60.+e, 25.70.Gh

I. INTRODUCTION

The discovery of new higher-Z elements and the determination of their decay properties provide important insights into our understandings of the behavior of nuclear matter under extreme conditions of high Z and important tests of the prediction of an island of stability around $N = 184$ and high Z (114 or even 120–126). The synthesis of odd-Z superheavy nuclei provides more detailed information than even-Z nuclei about the nuclear structure of these nuclides because of their longer decay chains as a result of strong fission hindrance caused by the unpaired nucleons. For the first time the $Z = 115$ nuclei and their odd-Z decay products including $Z = 113$ isotopes were observed in 2003 [1–4]. Three decay chains of $^{288}115 \rightarrow {}^{284}113 \rightarrow {}^{280}$Rg ... ^{268}Db and one decay chain of $^{287}115 \rightarrow {}^{283}113 \rightarrow {}^{279}$Rg ... ^{267}Db were discovered in the ^{243}Am(^{48}Ca,3–4n) complete-fusion reaction. In 2006 two decay chains of the lighter isotope ^{282}113 were synthesized in the ^{237}Np(^{48}Ca,3n) reaction [5]. The discovery of element 117 [6,7] has been reported using the ^{249}Bk + ^{48}Ca reaction; five decay chains of $^{293}117 \rightarrow {}^{289}115$ ... ^{281}Rg and one chain of the heaviest isotope $^{294}117 \rightarrow {}^{290}115$ ... ^{270}Db were observed in 2009–2010. A relatively high stability of all these odd-Z activities is caused by the influence of presumably spherical nuclear shells at $Z = 114$–126 and $N = 184$. The sequential α decays of the isotopes ^{282}113, ^{287,288}115, and ^{294}117 lead to $^{266–270}$Db ($N = 161$–165) that are already located in the vicinity of deformed nuclear shells at $Z = 108$ and $N = 162$.

For the synthesis and identification of these odd-Z nuclei, we used the Dubna Gas Filled Recoil Separator (DGFRS) that selects only complete-fusion-evaporation reaction products which are strongly forward peaked and suppresses the yield of transfer reactions and reactions with emission of charge particles (pxn, αxn, etc.). The energies of ^{48}Ca and measured reaction cross sections are comparable with results of experiments where excitation functions for the ^{242,244}Pu, ^{245,248}Cm + ^{48}Ca reactions have been measured (see Ref. [8] and references therein) and where the new elements 114 (Fl) and 116 (Lv) were discovered [9]. The excitation functions were measured at two ^{48}Ca energies in both reactions with ^{243}Am and ^{249}Bk. Use of larger projectile energies resulted in the production of lighter neighboring isotopes, namely $^{294}117 \rightarrow {}^{290}115$... and $^{293}117 \rightarrow {}^{289}115$... decay chains in the reactions with the ^{249}Bk target and $^{288}115 \rightarrow$ ... and $^{287}115 \rightarrow$ ... chains in the reactions with the ^{243}Am target, respectively. In full agreement with expectations, with an increase of neutron number of isotopes of the same element

*oganessian@jinr.ru

their α-particle energies decrease and half-lives become larger. The measured α-particle energies for all isotopes of odd-Z elements produced in the reactions ^{243}Am + ^{48}Ca and ^{249}Bk + ^{48}Ca agree well with the systematics of the α-decay energies of the heavy nuclei and have intermediate values between neighboring even-Z nuclei. The measured α-particle energies of the $Z = 107$ and $Z = 109$ isotopes as well as their behavior vs neutron number are in full agreement with what is observed for the neighboring lighter previously known nuclei. Moreover, ^{268}Db, the descendant nucleus of ^{288}115 and ^{284}113, was identified in independent chemistry experiments [4,10,11].

In addition to odd-Z nuclei with $Z > 111$ produced in the ^{48}Ca-induced reactions, three decay chains of the lightest $Z = 113$ isotope, ^{278}113, whose decay properties are governed by the deformed closed shells at $Z = 108$ and $N = 162$, were observed in the cold-fusion reaction ^{209}Bi(^{70}Zn,n) in 2004, 2005, and very recently in 2012 [12–14].

We have performed a new series of experiments to obtain more detailed information on the decay properties of odd-Z nuclei, to measure the excitation functions of the ^{243}Am + ^{48}Ca and ^{249}Bk + ^{48}Ca reactions at a more extended range of projectile energies, and to make a cross-bombardment consistency check on the reported discoveries of elements 113, 115, and 117 [1–4,6,7]. The first results of an ongoing experiment with ^{249}Bk target are given in Ref. [15]. Since April 23, 2012, we have observed five and two new decay chains of ^{293}117 and ^{294}117 activities, respectively. Here, in more detail, we present the synthesis of the $^{287-289}$115 isotopes in the ^{243}Am + ^{48}Ca experiments performed with a few breaks between November 1, 2010, and March 31, 2011 [16], and then between September 30, 2011, and February 26, 2012.

II. EXPERIMENT

The experimental setup is analogous to that used in our previous experiments [1–8,15,16]. The ^{48}Ca ion beam intensity of about 1 particle μA was obtained from the U400 cyclotron of the FLNR, JINR. The beam energy was determined with a systematic uncertainty of 1 MeV. We used 36 cm^2 targets of ^{243}Am (enrichment 99.5%–99.9%) deposited as oxides with three different thicknesses onto 1.5-μm Ti foils (see Table I). The evaporation residues (ERs) were separated from projectiles, scattered particles, and transfer-reaction products by the DGFRS with an estimated transmission efficiency for $Z = 115$ nuclei of about 35%, then passed through a time-of-flight system and implanted in a 4 × 12-cm detector with 12 vertical position-sensitive strips surrounded by eight 4 × 4-cm side detectors without position sensitivity. The detection efficiency for full-energy α particles from implanted nuclei was 87%.

The detection system was calibrated by registering the recoil nuclei and α decays or spontaneous fission (SF) fragments of known isotopes of No and Th and their descendants produced in the reactions ^{206}Pb(^{48}Ca,2n) and ^{nat}Yb(^{48}Ca,3–5n), respectively. The low-energy scale, used for registration of α particles and ERs, was calibrated by nine α lines of isotopes from ^{209}Rn ($E_\alpha = 6.04$ MeV) to ^{217}Th ($E_\alpha = 9.27$ MeV)

TABLE I. The ^{243}Am target thicknesses, laboratory-frame beam energies in the middle of the target layers, resulting excitation energy intervals, total beam doses, and numbers of observed decay chains assigned to the parent nuclei ^{287}115 (4n), ^{288}115 (3n), and ^{289}115 (2n) characterizing the studies presented in Ref. [16] and this work, are listed.

Target thickness (mg/cm^2)	E_{lab} (MeV)	E^* (MeV)	Beam dose $\times 10^{18}$	No. of chains 4n/3n/2n	Ref.
0.37	239.8	31.1–35.3	11.7	0/7/0	[16]
0.84	240.5	31.4–36.2	4.8	0/5/1	[16]
0.68	241.0	32.0–36.4	5.6	0/7/3	This work
0.37	243.4	34.0–38.3	3.3	0/6/0	[16]
0.37	248.1	38.0–42.3	3.7	0/3/0	[16]
0.68	253.8	42.5–47.2	4.4	1/0/0	This work

together with a precision pulse generator for the energy range up to about 20 MeV. The high-energy scale for detection of fission fragments was calibrated from the values determined for the α scale by means of a pulser and then the coefficients that were determined were additionally corrected by a few percent using the measured energies of ^{48}Ca scattered ions. The FWHM energy resolutions were 40–100 keV (depending on strip) for α particles absorbed in the focal-plane detector, 100–260 keV for α particles that escaped this detector with a low energy release and registered by a side detector, and 0.24–0.75 MeV for α particles detected only by a side detector (without a focal-plane position signal). The energy of the side-only events was estimated as the sum of the energy measured by the side detector and half of the threshold energy (1.0–2.0 and 0.5–0.6 MeV in the first and second run, respectively) with an uncertainty determined from the threshold energy and energy resolution of the side detector (68% confidence limit). The assignment of these α particles to the observed decay chains was made using the calculated probability of random correlations based on the decay rate in the side detectors associated with the actual experimental conditions. Fission fragments from the decay of ^{252}No implants produced in the ^{206}Pb + ^{48}Ca reaction were used for the total kinetic energy (TKE) calibration. The measured fragment energies presented in this work were not corrected for the pulse-height defect of the detectors or for energy losses of escaping fragments in the detectors and the pentane gas filling the detection system. The average sum energy loss of fission fragments from the SF decay of ^{252}No [17] was measured to be about 23 MeV.

The FWHM position resolutions of correlated ER-α and ER-SF signals were 1.1–1.6 and 0.5–1.0 mm, respectively. For α particles detected by both the focal-plane and side detectors, the ER-α position resolution depends on the energy deposited in the focal-plane detector and was, on average, 2.4–4.5 mm for energies lower than 3 MeV and 1.4–3.3 mm for energies larger than 3 MeV.

For detection of expected sequential decays of the daughter nuclides in the absence of beam-associated background, the beam was switched off for 2 min after the following conditions were observed: a recoil signal was detected with implantation energy $E_{ER} = 7$–16 MeV followed by an α-like signal in the focal-plane detector with an energy of $E_\alpha = 9.8$–11.0 MeV in the same strip, within a 2.4-mm-wide position window and time interval of $\Delta t_{\max} = 2.5 \times (11 - E_\alpha)$ s. If, during the first 2-min beam-off time interval, an α particle with $E_\alpha = 8.8$–10.8 MeV was registered in any position of the same strip, the beam-off interval was automatically extended to 6 min (both time intervals were two times lower in the experiments with thick targets of 0.68 and 0.84 mg/cm^2). During this beam-off period, if other α particles with energies expected for heavy nuclei were observed, we could prolong the beam-off pause further.

The experimental conditions and numbers of registered decay chain of ^{287}115, ^{288}115, and ^{289}115 are summarized in Table I. Excitation energies of the compound nuclei at given projectile energies are calculated using the masses of Refs. [18,19], taking into account the thickness of the targets and the energy spread of the incident cyclotron beam during long experiments. The beam energy losses in the separator's entrance window (0.74 mg/cm^2 Ti foil), target backing, and target layer were calculated using the nuclear data tables [20].

III. EXPERIMENTAL RESULTS

The results of the first experiment reporting the study of production and radioactive decay of nuclei with atomic number $Z = 115$, the properties of their daughter activities including the isotopes of element $Z = 113$, and the observation of the daughter activities of ^{293}117 nucleus [6,7] were presented concisely in an earlier publication [16].

In the second run the experimental studies of the formation of superheavy nuclei in the ^{243}Am + ^{48}Ca reaction and of their decay properties were continued at two beam energies: $E_{\rm lab} = 241.0$ MeV, corresponding to the excitation energy $E^* = 34.2 \pm 2.2$ MeV for ^{291}115 compound nuclei, and $E_{\rm lab} = 253.8$ MeV ($E^* = 44.8 \pm 2.3$ MeV).

At the lower ^{48}Ca beam energy, $E_{\rm lab} = 241.0$ MeV, seven long decay chains of the isotope ^{288}115 were detected. The energies of the α particles and the half-lives of the nuclei in these chains, as well as the energies of the fission fragments and the SF half-life, within statistical uncertainties and the energy resolution of the detectors, match the previously observed 24 decay events of ^{288}115 produced in the 3n-evaporation channel of the ^{243}Am + ^{48}Ca reaction [1–4,16]. In Table II, all observed decay chains of ^{288}115 are presented. The data listed in Ref. [16], seven events added in this work and three decay chains observed for the first time in the ^{243}Am + ^{48}Ca reaction at the beam energy of 248 MeV in 2003 [1–4] are shown. The long decay chain of ^{288}115 isotope is characterized by five subsequent α decays occurring within about 1 min and ending with a fission of ^{268}Db occurring within many hours after the last α transition ($T_{1/2} = 27$ h).

In this run, three other chains of the $\alpha \rightarrow \alpha \rightarrow$ SF type that last typically only about 30 s were also detected (Table III). Such a decay pattern is characteristic for the neighboring heavy isotope ^{289}115 that was observed for the first time as the α-decay daughter activity of the ^{293}117 isotope produced in the reaction ^{249}Bk(^{48}Ca,4n)^{293}117 [6,7,15] and later as an ER (single event) in the rare reaction channel ^{243}Am(^{48}Ca,2n)^{289}115 [16] (see lower part of Table III for comparison).

At the higher ^{48}Ca beam energy, $E_{\rm lab} = 253.8$ MeV ($E^* = 44.8 \pm 2.3$ MeV), we observed a single long decay chain of the ^{287}115 isotope. The decay properties of this chain, shown in Table IV, agree well with data recorded in the first experiment from 2003 [1–4]. The 2003 experiment was also performed at the energy $E^* = 45$ MeV. In both cases these events were attributed to the ^{287}115 isotope produced in the 4n-evaporation channel of the ^{243}Am + ^{48}Ca reaction [1–4]. Being the product of this channel, it could therefore not be observed in the ^{243}Am + ^{48}Ca reaction at lower energies.

Of all the 33 observed decay chains, only six chains were detected completely during beam-on intervals. In chain 4 (Table II) the ER energy exceeded an upper limit of 16 MeV; in chains 17 and 19, the α particles of parent nucleus ^{288}115 were detected by the both focal-plane and side detectors and ER-α_2 time intervals for ^{284}113 were larger than maximal correlation times for detected energies of 9.95 and 9.96 MeV; in chains 18 and 23 the α particles of ^{288}115 were detected by both the focal-plane and the side detectors and the α particles of ^{284}113 were missing. The ER-α_1 time interval in the third decay chain of ^{289}115 (Table III) was larger than the allowable value for $E_\alpha = 10.37$ MeV.

The spectrum of α-like signals (all events detected by the focal-plane detector or both the focal-plane and side detectors without a registered TOF signal) in all strips in the energy range $5.9 \leqslant E_\alpha \leqslant 12$ MeV accumulated during the 243-MeV ^{243}Am + ^{48}Ca experiment is shown in Fig. 1(a). The α-particle spectrum detected during beam-off time intervals is also shown in Fig. 1(a). In the high-energy part of the α-particle spectrum, where the decays of daughter nuclei ^{272}Bh to ^{284}113 ($E_\alpha = 8.7$–10.1 MeV) are expected, 79 events were detected with average counting rate of about 2/h. This demonstrates very low random probability for detection of 13 α particles (shown by arrows) which belong to the decays of the daughter isotopes of ^{288}115 (decay chains 20–25 in Table II) and occur within about a 1-min time interval after the decay of the parent nucleus. A similar spectrum of the fission-fragment-like signals, both beam on and beam off, measured under the same conditions, is shown in Fig. 1(b). In the energy range $E > 135$ MeV, the counting rate from the focal-plane detector was 0.2/h. Background conditions were comparable in all experiments. The calculated numbers of random sequences imitating each of the observed decay chains ranged from 2×10^{-3} to 10^{-14} [21].

As seen in Fig. 2(a), all of the signals of α and SF types following the signals of the ER implantation are in strict position correlation, which indicates that they belong to the decay of these implants. Three of four events with position deviations exceeding ± 1 mm were detected by both the focal-plane and the side detectors with low energy-release in the first event. The energies of all recoiling nuclei, except for those marked by footnote f (with their associated TOF signals), lie in the energy range $E_{\rm ER} = 8.2$–16.7 MeV [Fig. 2(b)], in agreement with the energy values measured for other superheavy nuclei produced in the ^{48}Ca-induced reactions with targets between ^{238}U and ^{249}Cf [1–8]. The comparison of energy spectra of the signals that terminate the decay chains shown in Tables II–IV (except for those marked by footnote e)

TABLE II. Observed decay chains originating from $^{288}115$. The first three columns show laboratory-frame beam energies in the middle of the target layers, decay-chain numbers, ER energies, and detector strip numbers. For the following decays the α-particle and SF fragment energies and the time intervals between events are shown. Bold events were registered during a beam-off period. The α-particle energy errors are shown in parentheses. Time intervals for events following a "missing α" were measured from preceding registered events and are shown in italic.

E_{lab} (MeV)	No.	E_{ER} (MeV) strip	$^{288}115$ E_α (MeV) t_α (ms)	$^{284}113$ E_α (MeV) t_α (s)	^{280}Rg E_α (MeV) t_α (s)	^{276}Mt E_α (MeV) t_α (s)	^{272}Bh E_α (MeV) t_α (s)	^{268}Db E_{SF} (MeV) t_{SF} (h)
239.8	1	8.20	Missing α[a]	9.944(54)	**9.721(54)**	**9.565(54)**	**9.028(54)**	173.5
		3		*0.8578*	**0.5844**	**0.0977**	**1.1824**	65.08
	2	12.38	10.495(62)	**10.07(75)**[b]	**9.48(69)**[b]	**9.599(62)**	**9.00(69)**	187.7[c]
		9	74.6	**2.3897**	**0.7483**	**1.2770**	**0.9725**	33.62
	3	12.20	10.527(56)	**10.32(59)**[b]	**9.724(206)**[d]	**9.77(59)**[b]	**8.977(56)**	216.3
		3	6.9	**2.5819**	**1.6542**	**0.1757**	**0.1669**	13.15
	4	16.66	10.345(65)	9.946(65)	9.783(65)	9.353(65)	9.130(217)[d]	221.4[c]
		9	36.0	1.2705	6.2185	1.1849	6.9108	14.75
	5	11.95	10.486(47)	**9.977(47)**	**9.825(47)**	**9.68(64)**[b]	**9.067(47)**	198.4
		4	30.4	**0.0216**	**3.2685**	**5.2044**	**12.0514**	61.28
	6	11.25	10.539(54)	**9.978(54)**	**9.64(63)**[b]	**9.948(54)**	**9.36(63)**[b]	**193.3**[c]
		11	1091.2	**0.0926**	**5.1057**	**0.7810**	**8.5397**	**29.11**
	7	11.82	10.427(62)	**10.42(69)**[b]	**9.521(62)**	**9.73(66)**[b]	**9.48(69)**[b]	**202.5**[c]
		7	7.268	**3.6278**	**4.5135**	**0.3489**	**11.1488**	**6.923**
240.5	8	10.21	10.521(62)	**9.939(62)**	**9.743(62)**	**9.607(62)**	**8.886(62)**	**210.2**[c,e]
		5	68.5	**0.3864**	**22.5392**	**0.4913**	**18.5325**	**9.82**
	9	10.48	10.496(62)	**9.951(62)**	**9.711(62)**	**9.450(62)**	**Missing α**[a]	135.1[e]
		5	768.0	**1.3436**	**0.4498**	**1.1404**		*7.036*
	10	12.11	10.558(50)	**9.973(50)**	**9.865(50)**	**9.26(64)**[b]	**Missing α**[a]	211.9[c]
		4	33.3[f]	**0.9648**	**4.4483**	**13.6480**		*43.60*
	11	10.28	Missing α[a]	9.977(63)	**10.00(58)**[b]	**9.629(63)**	**Missing α**[a]	205.1[c,e]
		6		*1.3435*	**6.6457**	**0.1447**		*23.07*
	12	11.81	Missing α[a]	9.978(61)	**9.749(61)**	**9.887(61)**	**Missing α**	189.3[c]
		5		*1.0732*[f]	**6.5550**	**0.6901**		*3.348*
241.0	13	11.72	10.483(65)	**9.988(65)**	**9.086(65)**	**9.46(24)**[b]	**9.032(65)**	166.8[c]
		5	136.3	**1.0180**	**4.3366**	**2.5596**	**16.9763**	67.48
	14	13.96	10.484(155)[d]	9.814(67)	**9.783(67)**	**9.529(67)**	**9.063(154)**[d]	135.0[e]
		8	13.937	0.4674	**5.8573**	**0.2094**	**17.4326**	17.40
	15	10.94	10.459(67)	**9.842(156)**[d,g]	**9.809(154)**[d,g]	**Missing α**	**9.030(67)**	204.8
		8	709.3	**4.9922**	**13.9813**		*2.2311*	15.45
	16	12.45	10.379(160)[d]	9.944(71)	**9.510(155)**[d,g]	**Missing α**	**9.011(71)**	204.5
		7	150.7	0.9508	**0.9111**		*22.5450*	11.15
	17	12.52	10.440(156)[d]	9.950(67)	9.728(67)	9.558(67)	8.925(67)	211.4[c]
		8	110.0	2.7645	2.0739	1.1736	41.2367	26.35
	18	10.25	10.446(160)[d]	Missing α	9.723(72)	9.404(122)[d]	8.725(72)	207.0
		6	358.4		*7.1451*	0.3735	107.5476	35.78
	19	12.45	10.438(152)[d]	9.960(72)	9.746(72)	9.166(72)	8.966(136)[d]	195.4
		6	188.5	2.4272	10.6749	0.0493	1.4956	7.18
243.4	20	13.26	10.326(76)	**9.929(76)**	**9.64(49)**[b]	**9.509(76)**	**9.044(76)**	170.3
		4	667.7	**0.7634**	**3.6829**	**0.5420**	**31.2979**	77.93
	21	9.74	10.378(86)	**9.983(86)**	**9.45(46)**[b,g]	**Missing α**	**9.012(86)**	**183.8**[c]
		6	66.4	**0.0447**	**7.3906**		*4.1337*	**12.72**
	22	10.26	10.479(94)	**9.748(153)**[d]	**9.728(94)**	**9.13(38)**[b]	**8.959(94)**	150.0
		7	37.7	**1.4083**	**2.8829**	**0.1803**	**1.6143**	103.97
	23	12.51	10.364(188)[d]	Missing α	9.733(76)	9.811(76)	9.009(76)	226.0[c]
		4	188.8		*0.6885*	16.9414	18.2305	9.23
	24	9.32	10.578(81)	**9.868(164)**[d]	**9.672(81)**	**9.565(81)**	**9.09(41)**[b]	150.1
		2	118.0	**5.2051**	**0.9438**	**0.9024**	**3.6080**	43.78
	25	11.30	Missing α	10.009(75)	**9.95(50)**[b]	**9.925(75)**	**9.012(75)**	219.8[c]
		1		*0.4072*	**1.6788**	**0.0380**	**0.3827**	41.33

TABLE II. (*Continued.*)

E_{lab} (MeV)	No.	E_{ER} (MeV) strip	^{288}115 E_α (MeV) t_α (ms)	^{284}113 E_α (MeV) t_α (s)	^{280}Rg E_α (MeV) t_α (s)	^{276}Mt E_α (MeV) t_α (s)	^{272}Bh E_α (MeV) t_α (s)	^{268}Db E_{SF} (MeV) t_{SF} (h)
248.1	26	11.48	10.534(103)	**9.967(156)**[d]	**9.826(103)**	**10.012(217)**[d]	**9.149(103)**	217.3[c]
		10	94.2	**0.9001**	**15.8352**	**2.8093**	**18.8541**	97.50
	27	13.08	10.498(86)	9.970(86)	**9.745(86)**	**9.805(86)**	**8.91(44)**[b]	196.0
		6	238.4	1.3435	**3.3038**	**0.4938**	**36.9231**	20.55
	28	11.85	10.430(76)	**9.83(49)**[b,g]	**9.672(76)**[g]	**missing α**	**8.948(153)**[d]	141.1
		4	879.0	**0.3662**	**1.7901**		*4.7246*	99.78
Decay chains of ^{288}115 observed in the first experiment in 2003 [1–4]								
248	1	10.39	10.506(70)	**10.043(185)**[d]	**9.718(70)**	**9.654(70)**	**9.23(61)**[b]	205.0[c]
		2	80.3	**0.3757**	**3.1457**	**1.0548**	**24.1028**	28.69
	2	10.98	10.380(62)	**9.48(61)**[b]	**9.755(62)**	**9.80(61)**[b]	**9.023(62)**	199.5[c]
		3	18.6	**1.1961**	**10.5988**	**0.2487**	**2.9635**	23.54
	3	9.09	10.497(54)	**9.999(54)**	**9.755(54)**	**9.744(54)**	**8.967(152)**[d]	140.0
		4	279.8	**0.5172**	**1.7927**	**1.8336**	**15.3880**	16.80

[a]Escaped α particle was registered by side detector only but probability of its random origin exceeds 10% [21].
[b]Escaped α particle registered by side detector only.
[c]Fission event registered by both focal-plane and side detectors.
[d]α particle registered by both focal-plane and side detectors.
[e]Another SF event was detected in the same strip and close position during next 6 days after last α decay.
[f]Another ER event was detected in the same strip and close position within 5 s preceding to α decay.
[g]Tentative assignment; α particles might originate from lower Z nuclei such as ^{280}Rg and ^{276}Mt.

with the sum energy spectrum of the fission fragments of ^{252}No measured in calibration reaction demonstrates that their sum energy is about 30 MeV higher than that characteristic of the SF decay of ^{252}No [17] and indicates the fission of very heavy nuclei.

The α-particle energy spectra of the isotopes observed in the decay chains originating from the parent nuclei ^{289}115 and ^{288}115 registered by the focal-plane detector in Refs. [1–4,6,7,15,16] and this work are summarized in the left-hand side of Fig. 3. The decay-time distributions on a logarithmic scale for the same isotopes are given on the right-hand side of Fig. 3 except for events followed after unobserved precursors or for which detection probabilities as random events exceeded 10% (three beam-on and three beam-off decays of ^{288}115 and ^{272}Bh, respectively, all registered by the side detector only, as well as four SF events of ^{268}Db).

For the first decay chain of ^{289}115 (Table III), two ER-like events with ER-α time intervals of 256 and 836 ms were detected in the same strip and close position within 5 s preceding to α decay with $E_\alpha = 10.377$ MeV. In calculating the half-life for this isotope, average decay time was used in addition to 10 other lifetimes measured in Refs. [6,7] (three events), [16] and this work (a total of four events including this one), and Ref. [15] (four events). In three decay chains

TABLE III. The same as Table II but for ^{289}115. The data on ^{289}115 daughter activity of ^{293}117 nucleus listed in the last row were taken from Refs. [6,7,15].

E_{lab} (MeV)	No.	E_{ER} (MeV) strip	^{289}115 E_α (MeV) t_α (ms)	^{285}113 E_α (MeV) t_α (s)	^{281}Rg E_{SF} (MeV) t_{SF} (s)
240.5	1	11.38	10.377(62)	**9.886(62)**	**215.7**
		3	256.2[f]	**1.4027**	**1.9775**
241.0	2	15.18	10.540(123)[d]	9.916(72)	**214.9**[c]
		6	66.1	1.5500	**2.3638**
	3	9.04	10.373(50)	9.579(50)	141.1
		2	2350.7	22.5822	60.1855
	4	13.35	10.292(170)[d]	10.178(55)	**182.2**[c]
		11	53.6	0.4671	**0.0908**
Decay chains of ^{289}115 observed after α decay of ^{293}117 [6,7,15]					
	1–10	9.36–13.51	10.20–10.37	9.36–9.86	
			17.5–1435.	0.24–18.40	1.48–103.4

TABLE IV. The same as Table II but for $^{287}115$.

E_{lab} (MeV)	No.	E_{ER} (MeV) strip	$^{287}115$ E_α (MeV) t_α (ms)	$^{283}113$ E_α (MeV) t_α (s)	^{279}Rg E_α (MeV) t_α (s)	^{275}Mt E_α (MeV) t_α (s)	^{271}Bh E_α (MeV) t_α (s)	^{267}Db E_{SF} (MeV) t_{SF} (h)
253.8	1	9.78 9	10.593(60) 45.2	**Missing α**	**10.391(163)**[d] ***0.1238***	**10.359(60)**[d] **0.0218**	**9.350(162)**[d] **1.7818**	192.8[c] 3.405
Decay chain of $^{287}115$ observed in the first experiment in 2003 [1–4]								
253	1	12.19 7	10.590(94) 46.6	**10.115(94)** **0.1474**	**10.365(163)**[d] **0.2450**	**10.329(94)** **0.0140**	**Missing α**	205.9[c] *1.766*

of $^{293}117$ [6,7,15], the α particles of $^{289}115$ were missing and the decay times of $^{285}113$ were measured after decays of the parent nucleus $^{293}117$. The half-lives of $^{289}115$ and $^{285}113$ differ by a factor of about 15 (see Fig. 3). So, in these 3 cases of all 12 observed, the decay times of $^{285}113$ were reduced by the average lifetime of $^{289}115$ for calculation of the $^{285}113$ half-life.

The radioactive decay properties of $^{288}115$ and $^{284}113$ discovered in 2003 [1–4] were completely confirmed by registration of 28 new decay chains in the new series of experiments (Ref. [16] and this work). One can see in Fig. 3 that the results of the three events in the first experiment, as indicated by vertical lines, are in good agreement with the extensive data of the recent work.

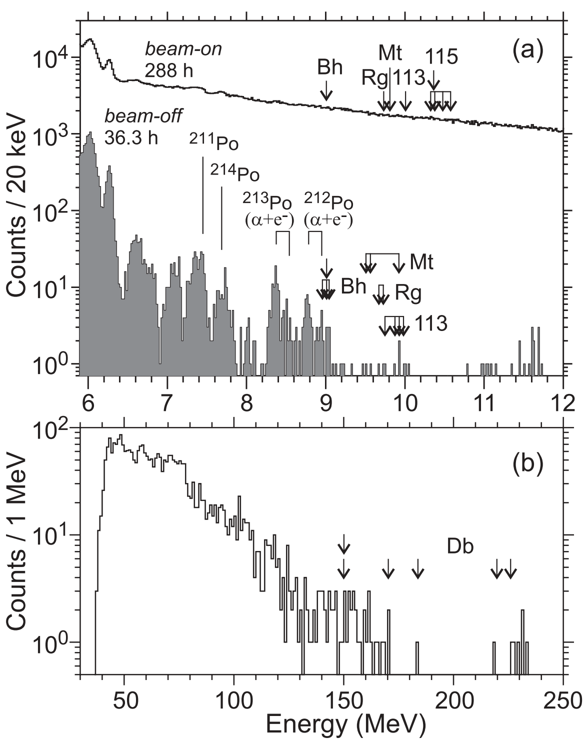

FIG. 1. (a) Total energy spectra of beam-on α-like signals and beam-off α particles recorded during the 243-MeV ^{243}Am + ^{48}Ca run. (b) Total fission-fragment energy spectrum. The arrows show the energies of events observed in correlated decay chains; see event numbers 20–25 in Table I.

In chain 25 (Table II) between the ER and the α particle with $E_\alpha = 10.009$ MeV, an event with $E_\alpha = 9.161$ MeV was observed in the same strip ($\Delta t_{ER-\alpha} = 0.298$ s, $\Delta P_{ER-\alpha} = 0.55$ mm) with an energy seemingly too low for $^{288}115$ (see Fig. 3). One cannot exclude that this particle deposited the main part of full energy in the focal detector and escaped from it at a small angle but the remaining part (~1.3 MeV) was lost in the

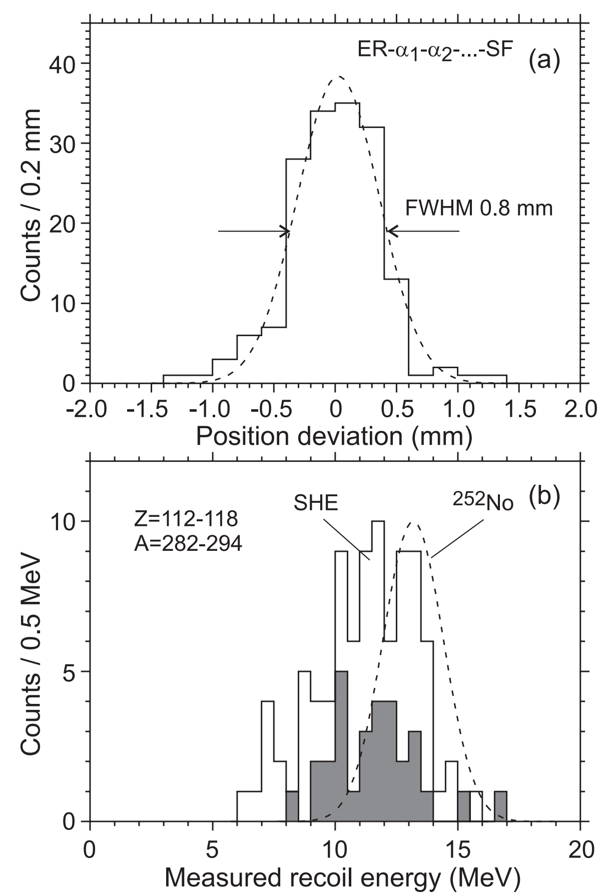

FIG. 2. (a) Relative position deviations of all events given in Tables II–IV (histogram) with a Gaussian fit (FWHM = 0.8 mm, dashed line). (b) Energy spectrum of all ERs with $Z = 112$–118 produced in ^{48}Ca-induced reactions [1–8]. The energy distribution of ^{252}No implants measured in the calibration reaction ^{206}Pb + ^{48}Ca is shown by the dashed line for comparison. Energies of $Z = 115$ ERs are shown by the gray histogram.

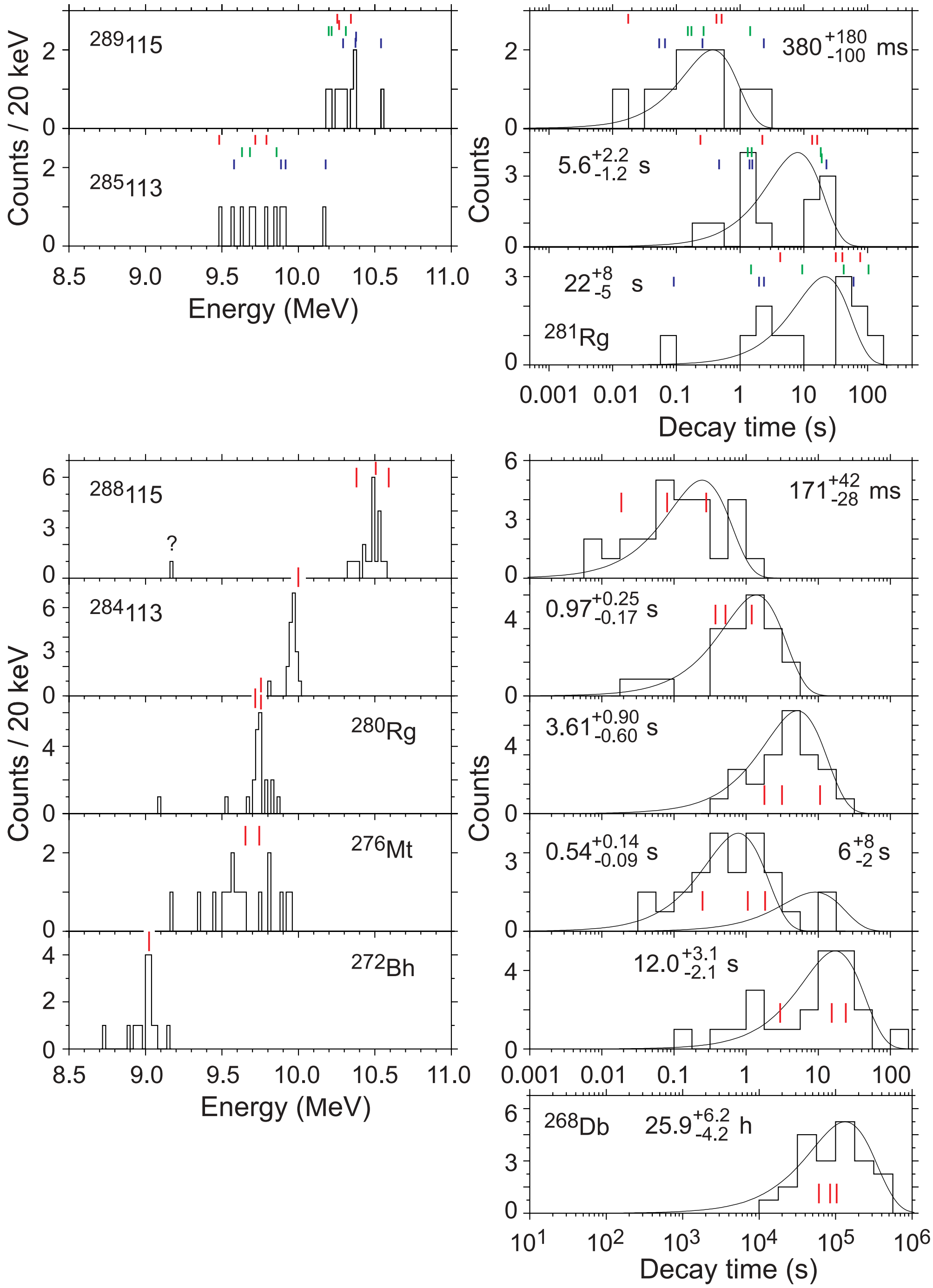

FIG. 3. (Color) α-particle energy spectra registered by the focal-plane detector (left-hand panel) and decay-time distributions on a logarithmic scale (right-hand panel) for isotopes originating from ^{289}115 and ^{288}115. The events originating from ^{289}115 observed in the reactions with ^{249}Bk in the first experiment [6,7], in the second experiment [15], and in the reaction with ^{243}Am (Ref. [16] and this work) are shown in the histograms by red (top), green (middle), and blue (bottom) lines, respectively. The red lines for nuclei in the decay chains of ^{288}115 show the energies and decay times of the three events obtained in the first experiment in 2003 [1–4]. The smooth curves are the time spectra for exponential decays associated with the half-lives $T_{1/2}$ shown in the figures.

dead layer or was not registered by the side detector. However, the probability is low for this occurrence ($\sim$0.003), and the probability of random appearance of this event is low as well ($\sim$0.002). With the large number of observed α decays (138 α particles) in this work, the chance to observe such an event is $N_{\rm err} \sim 0.3$–0.4.

Despite the limited statistics of these decay chains, one can see multiline α-particle energy spectra for ^{288}115, ^{280}Rg, and ^{272}Bh, which can be partially explained by the detection of conversion electrons in coincidence with α particles. An especially wide spectrum was observed for ^{276}Mt. At the same time, most of the α decays of ^{284}113 look like a transition from its one energy level to only one level of ^{280}Rg. Such a feature of the α-decay energy structure in this region of nuclei might be caused by theoretically predicted shape changes from oblate to prolate or from superdeformed to low prolate shapes (see, e.g., Refs. [22–24]) in the course of consecutive α decays. Irrespective of the α-particle energy spectra, the nuclei in the decay chains are characterized in practically all cases by a single half-life, as shown in the right-hand side of Fig. 3. The only exception is the decay of ^{276}Mt that shows the most complex α-particle spectrum; here one cannot exclude that two states with different lifetimes were observed. The average lifetime of the main part of events was about 0.8 s, whereas in a few cases (e.g., events No. 5, 10, 13, 23, 26 in Table II) the decay times were 2.5–17 s.

The observation of four decay chains of the heavier isotope ^{289}115, the product of the $2n$-evaporation channel, confirms the discovery of element 117 in the reaction with ^{249}Bk [6,7]. Note that the products of the $2n$ channel of the reactions of the fusion of ^{242}Pu and ^{245}Cm with ^{48}Ca, the isotopes ^{288}Fl and ^{291}Lv, were observed in our experiments with comparable cross sections at excitation energies of about 32–38 MeV [25–27].

The radioactive decay properties of isotopes ^{289}115, ^{285}113, and ^{281}Rg are shown on the top part of Fig. 3. Here data produced in the ^{249}Bk + ^{48}Ca reaction in the first experiment [6,7] are given by red vertical lines, data of Ref. [16] and this work by green lines, and results of the second experiment with ^{249}Bk target [15] by blue lines. One can see that the α-particle energies and the decay times of all of these nuclei have comparable values. Also, one can see a difference between isotopes originating from ^{289}115 and ^{288}115: (a) namely the half-lives of all three nuclides ^{289}115, ^{285}113, and ^{281}Rg are larger than those for lighter neighbors; (b) a difference is particularly evident for daughter nuclei ^{284}113, for which practically one line in the energy spectra was observed, and ^{285}113, for which a rather broad energy interval was detected even for low statistics; and (c) different decay modes were observed for ^{280}Rg (α decay) and ^{281}Rg (SF). In addition, in the ^{243}Am + ^{48}Ca reaction the isotope ^{289}115 was seen at the lowest projectile energy only. Because of the mass difference between ^{243}Am and ^{249}Bk the same isotope of element 115 in both these reactions can be produced only in the $2n$- and $4n$- evaporation channels of the ^{243}Am + ^{48}Ca and ^{249}Bk + ^{48}Ca reactions, respectively. Therefore, the isotope ^{289}115 was produced in cross reactions with two target nuclei ^{243}Am and ^{249}Bk to provide cross-bombardment evidence for the discovery of the new elements 113, 115, and 117.

Finally, at the highest ^{48}Ca energy, we observed only one ^{287}115 nucleus, the product of the $4n$-evaporation channel. Here, the α-decay energy and lifetime of ^{271}Bh were detected for the first time. The decay properties of all nuclei in the decay chain of ^{287}115 measured in this work are in full agreement with those observed in 2003 [1–4].

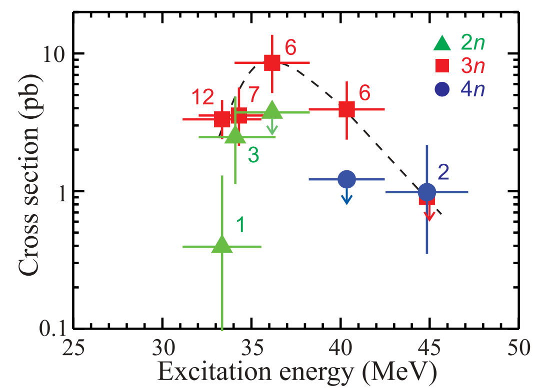

FIG. 4. (Color) Cross sections for the $2n$, $3n$, and $4n$ evaporation channels for the ^{243}Am + ^{48}Ca reaction. Vertical error bars correspond to statistical uncertainties [21]. Horizontal error bars represent the range of excitation energies populated at one beam energy. Symbols with arrows show upper cross-section limits. Numbers of detected decay chains are given for each ^{48}Ca energy. The dashed line through the $3n$ data are drawn to guide the eye.

Experimental values of the cross section for the production of the isotopes of element 115 measured in the ^{243}Am + ^{48}Ca reaction at various excitation energies of the compound nucleus, ^{291}115, are given in Fig. 4. When determining cross sections in the experiments with the 0.68 and 0.84 mg/cm^2 targets, we corrected the separator's transmission for increased scattering losses in the target. In calculations of the cross sections in both these cases we used 35% transmission for the effective target thickness of 0.4 mg/cm^2. We assumed that the first part of the thick target just reduces the ^{48}Ca beam energy and the ERs produced in this layer would not be able to reach the focal-plane detectors [28]. For two runs at $E^* = 33$ MeV (first 12 decay chains in Table II) we present summary cross-section values, as it was given in Ref. [16]. The cross sections for the $3n$- and $4n$-evaporation channels at 40- and 45-MeV excitation energies, respectively, were calculated taking into account results of the earlier experiments [1–4]. As one can see in Fig. 4 and in Tables II–IV, at the minimum excitation energy in the range of $E^* = 31.1$–36.4 MeV, we detected 19 decays of ^{288}115 nuclei and 4 decays of ^{289}115 nuclei. The corresponding cross sections for the formation of ERs in the $3n$- and $2n$-evaporation channels are about $3.5^{+2.7}_{-1.5}$ pb and $2.5^{+2.7}_{-1.5}$ pb, respectively. At energies $E^* \geqslant 36$ MeV, as it could be expected for the $2n$-evaporation product, ^{289}115 was not detected. This result agrees well with the previously measured excitation functions of the ^{242}Pu(^{48}Ca,$2n$)^{288}Fl [25] and ^{245}Cm(^{48}Ca,$2n$)^{291}Lv [26,27] reactions.

The cross section for the $3n$-evaporation channel reaches its maximum $\sigma_{3n} = 8.5^{+6.4}_{-3.7}$ pb at $E^* = 34.0$–38.3 MeV and decreases with further increase of the excitation energy of the compound nucleus ^{291}115. At the excitation energy, $E^* = 44.8 \pm 2.3$ MeV, not a single event indicating the formation of ^{288}115 was detected. The upper cross-section limit can thus be set at the level $\sigma_{3n} \leqslant 1$ pb. Generally, the behavior of the production cross section of ^{288}115 agrees well with the calculated dependence $\sigma_{3n}(E^*)$ [29] and experimental data which have been accumulated in previous experiments on the

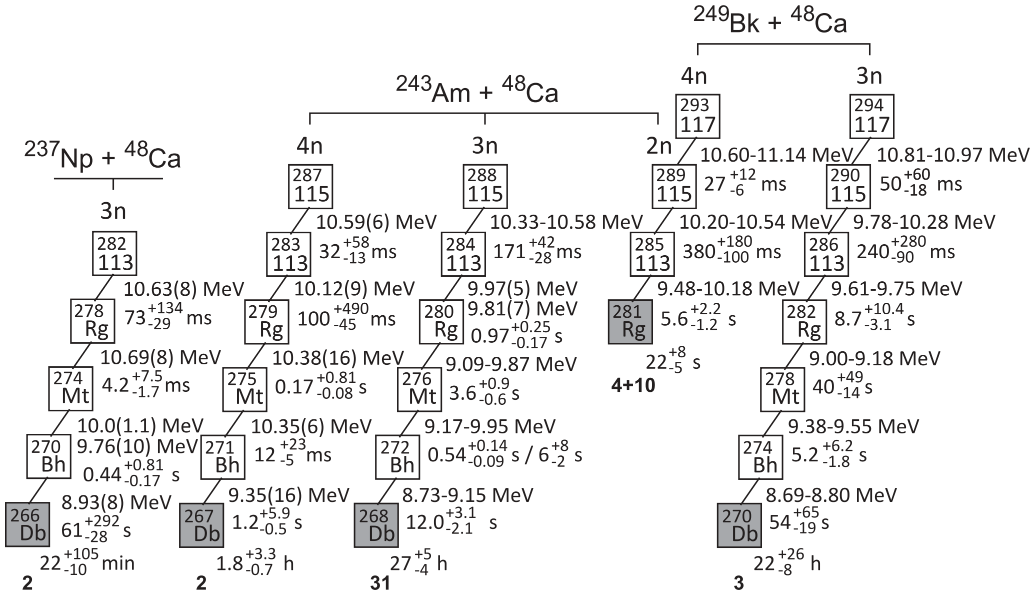

FIG. 5. Summary decay properties of the isotopes of elements 113, 115, and 117 observed for the first time among the products of ^{48}Ca beam and ^{237}Np, ^{243}Am, and ^{249}Bk target reactions. The number of the detected decay events of a given isotope is shown at the bottom of the chains. The energies of the emitted α particles and half-lives are given for all 23 new α emitters observed in these experiments. For five new spontaneously fissioning nuclei marked by gray squares, that is, the isotopes of Db and Rg that terminate the α-decay sequences with SF, the half-lives are listed. The value for ^{268}Db was obtained combining the results of Refs. [1–4,10,11,16] and those of the present work.

synthesis of ^{287}Fl and ^{290}Lv isotopes in the ^{242}Pu(^{48}Ca,3n) [25,30,31] and ^{245}Cm(^{48}Ca,3n) [26,27] reactions, respectively. The measured production cross sections of isotopes of element 115, $^{287-289}$115, with different decay properties, depending on ^{48}Ca beam energy, establishes that these events are the products of the 2n-, 3n-, and 4n-evaporation channels.

The decay sequences of the isotopes of elements 115 and 113 produced in the ^{243}Am(^{48}Ca,2–4n)$^{289-287}$115 reactions are shown in Fig. 5. This figure also displays decay chains of the heaviest isotope ^{290}115, the daughter of the isotope of element 117 synthesized in the ^{249}Bk(^{48}Ca,3n)^{294}117 reaction [6,7,15] and a lighter isotope of element 113, ^{282}113, product of the ^{237}Np(^{48}Ca,3n) reaction [5].

IV. CONCLUSION

From the data of Refs. [1–4,16] and present work one can draw the following conclusions.

(i) Three isotopes of element 115 with masses 287, 288, and 289 have been synthesized in the ^{243}Am + ^{48}Ca reaction. Decay properties of ^{288}115, of all the daughter products of its sequential α decays as well as the SF of the terminal nucleus, ^{268}Db, agree with prior data [1–4]. The ^{288}115 isotope is produced most abundantly (total of 31 decay chains), with the highest cross section reaching $\sigma_{3n} = 8.5^{+6.4}_{-3.7}$ pb at $E^* \approx 36$ MeV. This value exceeds the production cross section of ^{278}113 in the cold-fusion reaction ^{209}Bi(^{70}Zn,n) by a factor of nearly 400 [14].

(ii) At the excitation energy $E^* \approx 34 \pm 2$ MeV of the compound nucleus ^{291}115, we have detected four decay chains of the ^{289}115 isotope, the product of the 2n-evaporation channel. Decay energies and half-lives of the nuclei in the $^{289}115 \rightarrow {}^{285}113 \rightarrow {}^{281}$Rg decay chains observed in the ^{243}Am + ^{48}Ca reaction agree within statistical uncertainties with the decay properties of the daughter nuclei of the ^{293}117 nucleus produced in the ^{249}Bk(^{48}Ca,4n)^{293}117 reaction (10 events) [6,7,15]. Such agreement provides independent identification and consistency checks via cross-bombardment production of the same nuclei in different fusion reactions of ^{243}Am and ^{249}Bk targets with ^{48}Ca projectiles.

ACKNOWLEDGMENTS

We are grateful to the JINR Directorate and U400 cyclotron and ion source crews for their continuous support of the experiment. We acknowledge the support of the Russian Foundation for Basic Research Grants No. 11-02-12050 and No. 11-02-12066. Research at ORNL was supported by the US DOE Office of Nuclear Physics under DOE Contract No. DE-AC05-00OR22725 with UT-Battelle, LLC. Research at Lawrence Livermore National Laboratory was supported by LDRD Program Project No. 08-ERD-030, under DOE Contract No. DE-AC52-07NA27344 with Lawrence Livermore National Security, LLC. This work was also supported by the US DOE through Grant No. DE-FG-05-88ER40407 (Vanderbilt University). These studies were performed in the framework of the Russian Federation/US Joint Coordinating Committee for Research on Fundamental Properties of Matter.

[1] Yu. Ts. Oganessian, Pure Appl. Chem. **76**, 1715 (2004).
[2] Yu. Ts. Oganessian *et al.*, Prog. Theor. Phys. Suppl. No. **154**, 406 (2004).
[3] Yu. Ts. Oganessian *et al.*, Phys. Rev. C **69**, 021601(R) (2004).
[4] Yu. Ts. Oganessian *et al.*, Phys. Rev. C **72**, 034611 (2005).
[5] Yu. Ts. Oganessian *et al.*, Phys. Rev. C **76**, 011601(R) (2007).
[6] Yu. Ts. Oganessian *et al.*, Phys. Rev. Lett. **104**, 142502 (2010).
[7] Yu. Ts. Oganessian *et al.*, Phys. Rev. C **83**, 054315 (2011).
[8] Yu. Ts. Oganessian, J. Phys. G: Nucl. Part. Phys. **34**, R165 (2007).
[9] R. C. Barber *et al.*, Pure Appl. Chem. **83**, 1485 (2011).
[10] S. N. Dmitriev *et al.*, Mendeleev Commun. **15**, 1 (2005).
[11] N. J. Stoyer *et al.*, Nucl. Phys. A **787**, 388c (2007).
[12] K. Morita *et al.*, J. Phys. Soc. Jpn. **73**, 2593 (2004).
[13] K. Morita *et al.*, J. Phys. Soc. Jpn. **77**, 045001 (2007).
[14] K. Morita *et al.*, J. Phys. Soc. Jpn. **81**, 103201 (2012).
[15] Yu. Ts. Oganessian *et al.*, Phys. Rev. Lett. **109**, 162501 (2012).
[16] Yu. Ts. Oganessian *et al.*, Phys. Rev. Lett. **108**, 022502 (2012).
[17] J. F. Wild *et al.*, J. Alloys Compd. **213/214**, 86 (1994).
[18] G. Audi, A. H. Wapstra, and C. Thibault, Nucl. Phys. A **729**, 337 (2003); G. Audi *et al.*, Chinese Phys. C **36**, 1157 (2012).
[19] W. D. Myers and W. J. Swiatecki, Nucl. Phys. A **601**, 141 (1996).
[20] F. Hubert, R. Bimbot, and H. Gauvin, At. Data Nucl. Data Tables **46**, 1 (1990).
[21] K.-H. Schmidt *et al.*, Z. Phys. A **316**, 19 (1984).
[22] S. Ćwiok, P.-H. Heenen, and W. Nazarewicz, Nature (London) **433**, 705 (2005).
[23] M. M. Sharma, A. R. Farhan, and G. Münzenberg, Phys. Rev. C **71**, 054310 (2005).
[24] M. Warda and J. L. Egido, Phys. Rev. C **86**, 014322 (2012).
[25] Yu. Ts. Oganessian *et al.*, Phys. Rev. C **70**, 064609 (2004).
[26] Yu. Ts. Oganessian *et al.*, Phys. Rev. C **69**, 054607 (2004).
[27] Yu. Ts. Oganessian *et al.*, Phys. Rev. C **74**, 044602 (2006).
[28] R. N. Sagaidak, V. K. Utyonkov, and F. Scarlassara, Nucl. Instrum. Methods Phys. Res. A **700**, 111 (2013).
[29] V. I. Zagrebaev, Nucl. Phys. A **734**, 164 (2004).
[30] L. Stavsetra *et al.*, Phys. Rev. Lett. **103**, 132502 (2009).
[31] P. A. Ellison *et al.*, Phys. Rev. Lett. **105**, 182701 (2010).